Early stages of disordering processes at the impact between rough surfaces: a molecular dynamics study

2006 J. Phys.: Condens. Matter 18 8723

(http://iopscience.iop.org/0953-8984/18/39/005)

INSTITUTE OF PHYSICS PUBLISHING JOURNAL OF PHYSICS: CONDENSED MATTER

J. Phys.: Condens. Matter **18** (2006) 8723–8736 doi:10.1088/0953-8984/18/39/005

Early stages of disordering processes at the impact between rough surfaces: a molecular dynamics study

F Delogu

Dipartimento di Ingegneria Chimica e Materiali, Università di Cagliari, piazza d'Armi, I-09123 Cagliari, Italy

E-mail: delogu@dicm.unica.it

Received 16 May 2006, in final form 4 July 2006
Published 11 September 2006
Online at stacks.iop.org/JPhysCM/18/8723

Abstract

Numerical calculations have been employed to study the mechanical deformation of two semi-crystals of different metallic species colliding at relatively low temperature. The roughness of the semi-crystal surfaces induces local shear events that mediate the formation of an interface between the two metallic species. The surface asperities represent the points of local contact between the semi-crystals. The atomic species located in such regions experience a sudden mechanical load and an unusual localization of kinetic energy, resulting in an enhancement of their mobility. Correspondingly, significant atomic migration processes take place at relatively high rates. Atomic mixing phenomena originated by the relative motion of the colliding surfaces are also observed at the interface. After the removal of mechanical loads, the atoms involved in interfacial displacement processes are not able to recover a crystalline structure and keep a disordered arrangement despite the occurrence of thermally induced relaxation processes.

(Some figures in this article are in colour only in the electronic version)

1. Introduction

The plastic deformation of crystalline phases involves the formation of planar, line and point defects and the related storage of excess mechanical energy [1–3], which enhances the chemical reactivity and eventually results in phase transformations [4–6]. These aspects underlie the methods of powder metallurgy exploiting a mechanical cold-working of powder particles [4–8]. At each processing event, a fraction of powder trapped between colliding surfaces experiences a severe mechanical load. Under such circumstances, a series of local shear events takes place on the microscopic scale [6–8] and considerable amounts of energy correspondingly localize in relatively small volumes of solid phase [9–20]. Complex aggregates of atoms with defective coordination appear during the period of mechanical loading, mediating the occurrence of mass transport and chemical mixing processes [17, 19, 20]. As a consequence

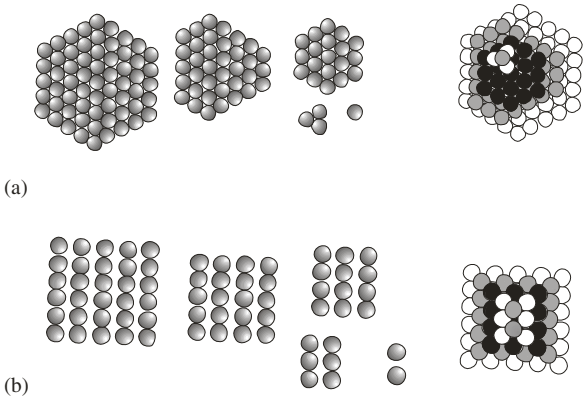

Figure 1. A schematic depiction of the structural motifs (right) and their simple components (left) employed to model the surface of the Ni (a) and of the Zr (b) semi-crystals. In the case of Ni, the atomic assembly includes 120 atoms. In the case of Zr, the structural motif is formed by 70 atoms.

of thermal equilibration, the above mentioned defective structures however relax and to a large extent disappear when the load is removed and the shearing interrupted [19, 20]. These evidences suggest a strong coupling between thermally and mechanically induced mechanisms of mass transport, establishing a connection between the conventional thermal diffusion scenarios [21–26] and the recent approaches based on 'interface roughening' and 'shear induced' processes [9–20]. The intimate mechanisms governing the mechanically induced processes are however still a matter of debate [6, 7] and the role of localized mechanical stresses and related excited states should be clarified [6, 7, 9–20].

Along such a line of inquiry, this work investigates by molecular dynamics the atomic-scale processes characterizing the early stages of the collision between two semi-crystals of different metallic species. Surfaces with pre-definite roughness were created to allow for the impact event to begin at selected surface asperities and properly analyse the response of crystals to local shear stresses. This preliminary study focuses on a particular morphology of the colliding surfaces and thus the results obtained are not expected to apply quantitatively to other cases. The numerical findings are however expected to throw light on the details of atomic displacement and mixing under mechanical loading, allowing further insight into the mechanistic framework explored in previous work [19, 20]. This also permits us to compare the response of the crystalline systems to different mechanical solicitations. The numerical methods employed are described in detail in the following section.

2. Computational outline

Calculations were carried out on a configuration of 36 315 atoms consisting of two semi-crystals of Ni and Zr. The relaxed semi-crystals were prepared separately and successively arranged in the space in order to obtain the desired configuration.

The Ni semi-crystal was prepared by starting from 17 100 Ni atoms arranged in the fcc cF4 structure with a stacking sequence of 19 (111) planes along the z Cartesian direction. The surface structure was arbitrarily constructed by employing the structural motif schematically depicted in figure 1(a). It consists of 120 atoms arranged on five atomic layers containing 61, 36, 19, three and one atoms respectively. Four identical assemblies of this kind were placed on the 19th atomic plane with orientations and positions keeping the fcc (111) stacking sequence

and avoiding any contact between the assemblies. The Ni semi-crystal was therefore formed by 17 980 atoms.

An analogous procedure was employed to generate the Zr semi-crystal. The starting configuration consisted of 18 125 Zr atoms, with the characteristic hcp hP2 structure and a stacking sequence of 29 (100) planes along the z Cartesian direction. The surface structure was modelled by means of the structural motif schematically illustrated in figure 1(b), consisting of 70 atoms arranged on five atomic layers containing 30, 20, 12, six and two atoms respectively. Three identical atomic assemblies of this kind were placed on the 29th atomic plane in order to keep the underlying crystalline order and avoiding any contact between the assemblies. The Zr semi-crystal consisted then of 18 335 atoms.

The number of atoms per side of the semi-crystals was selected in order to minimize the mismatch effects originating from the different sizes of the atomic species and the consequent different nearest neighbour distances.

Interatomic potentials were described by a semi-empirical tight-binding force scheme based on the second-moment approximation to the electronic density of states [27, 28]. The cohesive energy E was then equal to the summation of a repulsive Born–Mayer pair-wise interaction and of an attractive part expressed within the framework of the second-moment approximation of the tight-binding band energy [28, 29]. Interactions were computed within a cut-off radius approximately corresponding to the seventh shell of neighbours in Ni [27–30]. The values of the parameters of the interatomic potential were taken from the literature [27, 28].

The equations of motion were solved by employing a fifth-order predictor–corrector algorithm [31] with a time step δt equal to 2.0 fs.

The initial configuration of each semi-crystal was relaxed at 300 K for 0.1 ns. Periodic boundary conditions were applied along the x and y Cartesian directions. A 'reservoir region' of seven atomic planes was defined along the z Cartesian direction at one end of each semi-crystal, the free surface being located at the opposite end. Within each reservoir, the atoms belonging to the five atomic planes more distant from the free surface were considered immobile and occupied fixed positions defined by the ideal crystalline arrangement. The conventional Nosè–Hoover thermostat [32] was applied to keep the temperature T constant at 300 K. The Parrinello–Rahman scheme was also implemented to deal with eventual changes in the geometry of the elementary fcc and hcp crystallographic cells [33].

After the equilibration stage, the two semi-crystals were suitably positioned with the free surfaces facing each other at a distance of 0.4 nm. At such distance the atomic species at the semi-crystal surfaces do not significantly interact. The system configuration with the Ni semi-crystal placed above the Zr one along the z Cartesian direction is schematically illustrated in figure 2. A constant normal force F_n was then applied to the Ni reservoir atoms [10]. A centre-of-mass velocity was thus given to the Ni system along the z Cartesian direction. The intensity of the force was selected in order to obtain a relative velocity of collision between the two semi-crystals of about 10 m s^{-1}. Such a value was chosen in order to roughly reproduce the usual conditions of mechanical treatment in ball mills [6–8, 34], where the average impact velocity typically ranges between 2 and 14 m s^{-1}.

The beginning of the impact between the semi-crystals is defined as the instant in which Ni and Zr atoms approach to a distance smaller than the equilibrium distance between Ni and Zr atoms at 0 K. The simulation time t was suitably scaled to zero at the beginning of the collision event.

As the normal force F_n was applied, the Nosè thermostat was imposed only on the atoms in the reservoirs. This permitted us to avoid the stochastic coupling with a thermal bath during the course of the impact and to evaluate the spontaneous distribution of the kinetic energy between the atomic species located at the free surfaces or close to them. Reservoirs were kept

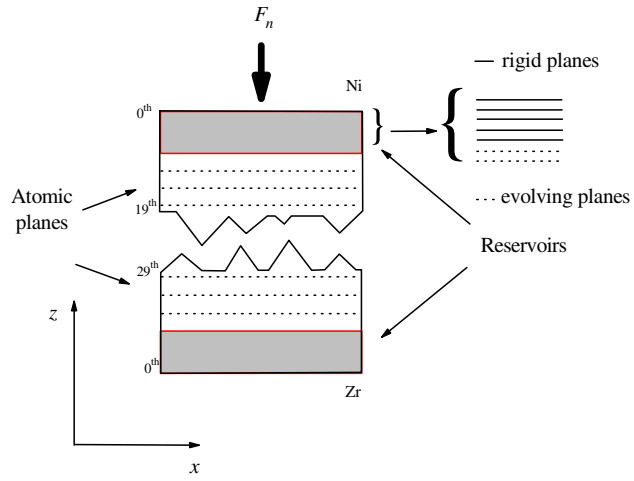

Figure 2. A schematic illustration of the simulation box. The two 'reservoir' regions are shown in grey at the borders of the simulation cell. The structure of the reservoir regions is shown in detail to indicate the five immobile and the two mobile atomic planes. The rough free surfaces are also schematically shown. A normal force F_n applies along the z Cartesian direction to the Ni semi-crystal.

at a constant temperature T of 300 K. The atoms not located within the reservoir regions were left free to move according to the Newton's equations of motion [31]. The temperature T was calculated according to the usual kinetic definition [31].

The long-range crystalline order in the atomic planes below the surface was quantified by means of the so-called planar static order parameter $S_p(\boldsymbol{k})$ [31], where the wavevector $\boldsymbol{k}$ is a reciprocal lattice plane vector. For an ideal crystal at 0 K, $S_p(\boldsymbol{k})$ equals unity for any wavevector $\boldsymbol{k}$. In a completely disordered plane it fluctuates instead near zero. $S_p(\boldsymbol{k})$ provides thus a direct quantitative measure of the degree of structural disorder in the system. In the present case, the degree of disorder was evaluated with reference to the crystallographic planes (111) and (100) for the Ni and Zr lattices respectively. The degree of structural order in the system was also monitored by means of the pair correlation function (PCF) $g(r)$ [31].

Structural defects were characterized by looking at those atoms, hereafter referred to as defective, characterized by a defective coordination. A defective atom is here defined as an atom with a number of nearest neighbours different from 12, the characteristic coordination number for fcc and hcp lattices. A distance criterion was adopted to check the number of nearest neighbours. In particular, two atoms were regarded as nearest neighbours when their distance was smaller than the distance r_m corresponding to the first minimum in the PCF. Given that the atoms at the surface have necessarily an incomplete coordination shell and therefore an intrinsic defective coordination, surface atoms were not included in the ensemble of defective atoms.

The above mentioned distance criterion can be applied when the proper length scale is used for each phase considered. The pure Ni and Zr phases have natural length scales $r_{m,Ni}$ and $r_{m,Zr}$. The further length scale $r_{m,mix}$ appears however at the collision event as a consequence of the shear-induced chemical mixing taking place at the interface. $r_{m,mix}$ depends on the relative concentration of Ni and Zr atoms in the considered region of solid and its evaluation requires first the estimation of the mixed interfacial layer thickness and then the calculation of the corresponding PCF. Once mixing has started, three different regions must therefore be distinguished to evaluate the atomic coordination numbers.

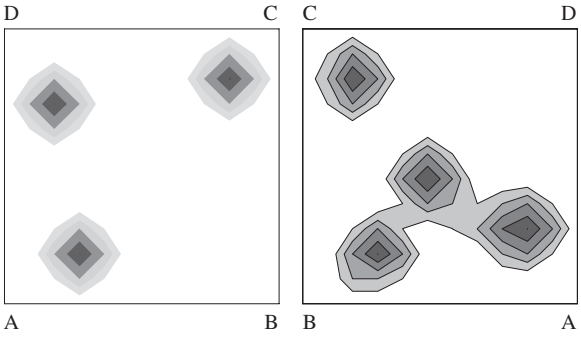

Figure 3. The projection of the surface structure on the $(x; y)$ plane for Ni (right panel) and Zr (left panel) semi-crystals. A density level map is used for the sake of clarity. The Ni and Zr semi-crystals are reciprocally oriented to let the same letters superpose when the surfaces are facing each other.

3. Structural evolution of the colliding semi-crystals on the atomic scale

An initial equilibration stage at 300 K, lasting 0.1 ns, allowed the single Ni and Zr semi-crystals to separately relax their starting atomic configurations. As expected, the atomic species at the free surfaces were the most mobile and underwent local displacements to attain as low as possible potential energy. Such behaviour is strictly connected with the degree of unsaturation of the coordination shells. Atomic species with a stable equilibrated coordination have 12 nearest neighbours. Surface atoms have instead an incomplete coordination shell, with the number of nearest neighbours depending on their position on the surface. For example, the Ni atoms on a plane portion of the surface (111) plane have nine nearest neighbours, whereas the Ni atoms on the top of the surface asperities have only three nearest neighbours. Analogous considerations hold for Zr surface atoms. The coordination number determines to a great extent the potential energy experienced by the single atoms. Given that the mobility of a given atom is roughly proportional to its potential energy, the surface atoms with the smallest coordination number are expected to have the highest mobility.

In a sense, a thermodynamic tendency to the minimization of the surface roughness formed by defectively coordinated atoms exists. Only short-range atomic displacements however took place in the present case and even the surface asperities did not undergo significant modifications. An extensive reconstruction of the free surfaces was indeed prevented by the low temperature, far from the equilibrium melting points T_m for the Ni and Zr chemical species [35].

The surface patterns obtained at the end of the initial equilibration stage are shown in figure 3. It can be seen that two of the four asperities at the Ni surface have a position approximately coincident with two of the three asperities at the Zr surface. Such Ni and Zr asperities then formed the points of first contact between the semi-crystals at impact.

3.1. The collision event

The normal force accelerating the Ni semi-crystal toward the Zr one was applied at the end of the initial equilibration stage and kept constant during the simulation of the impact event. Negligible configurational changes took place while the two relaxed semi-crystals approached, with only a few atomic displacements of Ni and Zr atoms at the top of the surface asperities ascribable to interactions between the semi-crystals.

As briefly mentioned above, the collision event initially involved two Ni and two Zr surface asperities. At the points of local contact, sudden mechanical loads developed, determining far-from-equilibrium conditions for the successive dynamical evolution. The atomic species located within the region of impact accumulated considerable atomic strain under the action of local shear stresses. To relieve at least partially such strain, the coordination shells and the

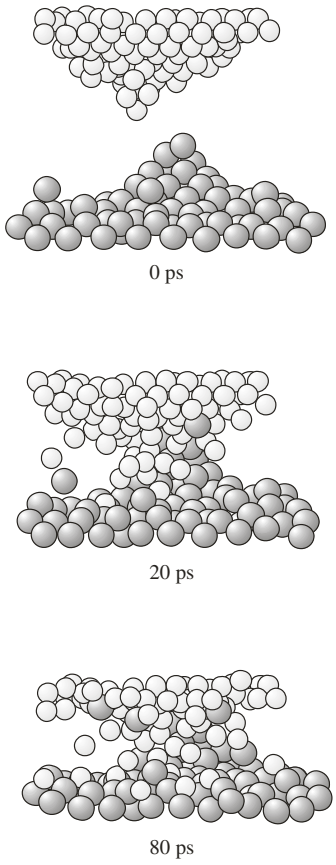

Figure 4. The atomic configurations of two colliding surface asperities at the times quoted. The structure of the asperities is drastically modified as the collision proceeds and surface atoms are heavily displaced from their positions. A small number of atoms is also projected in the vapour phase for small time intervals. Interfacial mixing induced by severe atomic rearrangements is also evident.

local atomic configurations underwent deep and fast modifications. The sequence of elementary processes taking place during the impact between two asperities can be intuitively rationalized looking at figure 4, where the atomic configurations are shown at different times. The atoms are highly displaced from their initial positions by local shear stresses that promote atomic mass transport under ballistic conditions, with a certain number of atoms also projected into the vapour phase. Such atoms move on approximately straight lines until they impact on either the Ni or the Zr surfaces. The migration of atoms under far-from-equilibrium conditions also results in a rapid mixing of atomic species with a mechanism completely different from the thermal diffusion and governed only by local shearing events.

The atomic species located in the regions of first contact acquire considerable kinetic energies as a consequence of the mechanical loads responsible for the local lattice deformation. Given the proportionality between kinetic energy and absolute temperature T, local temperature rises are observed. Of course, the instantaneous temperature does not correspond to the equilibrium temperature defined by the zeroth principle of thermodynamics [36]. The distributions of the Ni and Zr surface temperatures were obtained by considering the Ni atoms belonging to the 19th plane or located between it and the 29th plane of the Zr semi-crystal and the Zr atoms belonging to the 29th atomic plane or located between it and the 19th plane of the Ni semi-crystal. The simulation cell was then divided into a grid of 144 cells. The kinetic energy of the surface atoms belonging to each cell was then averaged over the atoms located within the cell and the corresponding kinetic temperature evaluated.

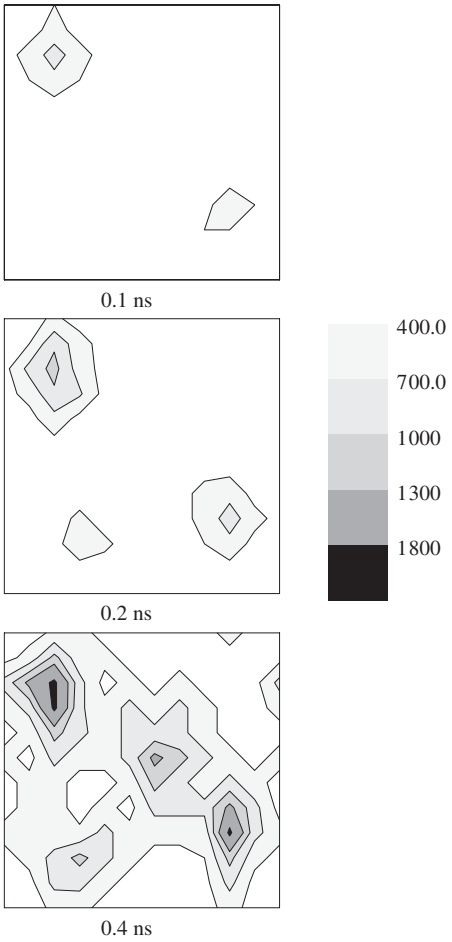

Figure 5. The temperature distribution at the Ni/Zr interface at the times quoted. The projection on the $(x; y)$ plane of the distribution is shown. The distribution was obtained by referring to a grid of 12×12 two-dimensional cells and averaging the temperature over the surface atoms contained in each cell. Temperatures as high as 2100 K are attained in correspondence of the surface asperities. The temperature coding with grey levels is also shown.

The two-dimensional temperature distributions at the Ni/Zr interface at different times are shown in figure 5. The temperatures of the regions of first contact are considerably higher than the ones in the rest of the surface. The kinetic energy of the atomic species located within such regions or adjacent to them increases markedly as the collision proceeds, enhancing the mobility of an increasing number of surface atoms. Correspondingly, the temperature rise gradually spreads over the whole semi-crystal surface. Temperature distributions also indicate that local temperatures undergo rapid variations, with an irregular dynamics due to the underlying highly disordered behaviour of surface atoms.

The apparent temperature can locally attain values as high as 2100 K, i.e. values about 500 K above the estimated equilibrium melting point of a Ni system and about 300 K above the one of a Zr system. Such hot spots at the surface of the two semi-crystals can be regarded as small regions of volume in which the Ni and the Zr lattices collapse as a consequence of a local melting. The melting process is not only local, but also transient. It appears indeed that the very high temperatures associated with a certain number of hot spots are observed for very short time periods, with a duration on the order of 20 ps. It is however worth remembering that the local failure of the crystalline arrangement is not a consequence of thermal phenomena, but rather of the localization of kinetic energy due to the action of shear stresses.

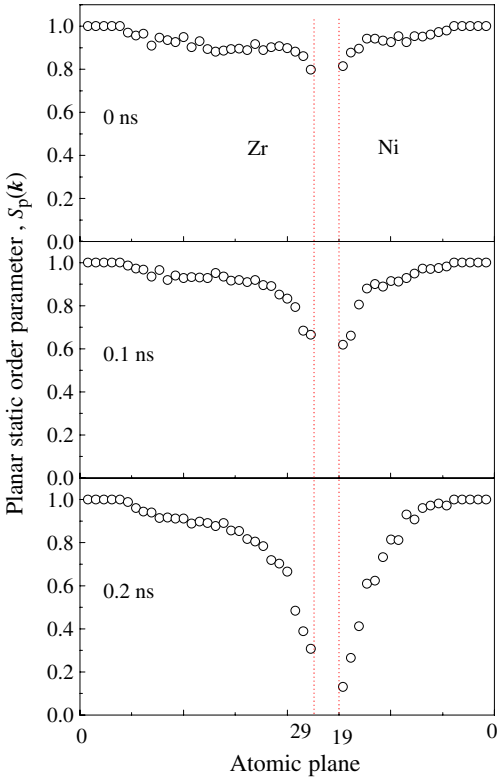

Figure 6. The planar structure factor $S_p(k)$ for the different atomic planes at the times reported. Initial values smaller than unity are a consequence of the thermal vibrations of atoms around their equilibrium lattice positions. Markedly lower $S_p(k)$ values are observed successively starting from the 19th Ni and the 29th Zr atomic planes, pointing out a loss of structural order connected with the propagation of the mechanical deformation below the surface. The propagation takes place at a rate of about 100 m s^{-1}.

3.2. Below the surface

Although the collision event involves initially only surface atoms, the mechanical deformation rapidly propagates at the underlying atomic layers. The propagation of the mechanical deformation and of the associated disordering phenomena below the surface layer was followed by means of the planar static order parameter $S_p(k)$, calculated for the 19 Ni atomic planes and for the 29 Zr ones. The $S_p(k)$ values are shown in figure 6 for different times. At the beginning of the impact event, when the atoms at the top of the surface asperities of Ni and Zr semi-crystals did not yet significantly interact, all the atomic planes have $S_p(k)$ values only slightly smaller than unity as a consequence of the thermal vibrations of atomic species around their equilibrium lattice positions. Of course, the $S_p(k)$ parameter amounts exactly to unity for the five planes consisting of immobile atomic species in the Ni and Zr reservoirs. Starting from the 19th Ni and the 29th Zr atomic planes, the mechanical deformation propagates at a rate of about 100 m s^{-1} and a gradual disordering takes place as the collision proceeds.

The gradual disordering is due to the formation of atoms with a defective coordination. The atoms referred to as defective have a number of nearest neighbours different from 12, the equilibrium number for fcc and hcp lattices. As mentioned before, surface atoms also have a defective coordination. In this case, the defective coordination is however intrinsic. For this reason, surface atoms will not be included in the ensemble of defective atoms formed as a result of the action of shear stresses. Also the immobile atoms in the reservoir regions will not be considered. Accordingly, in the case of Ni defective atoms will be hereafter defined as the atoms with defective coordination initially located in the region between the sixth and the 18th

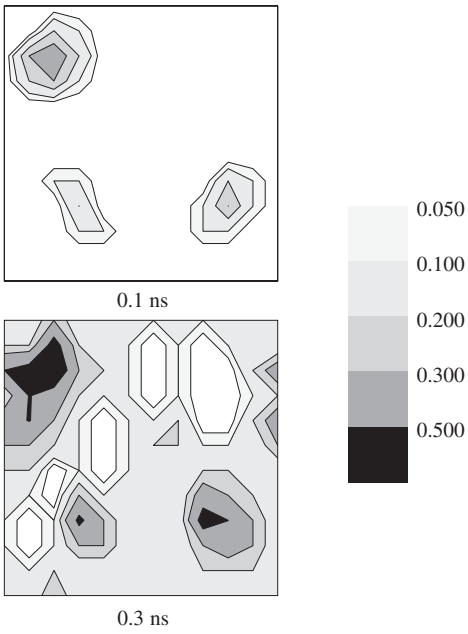

Figure 7. The two-dimensional distribution of Ni and Zr defective atoms. The distribution is obtained by projecting onto the $(x; y)$ plane the positions of defective atoms irrespective of their z Cartesian coordinates after 0.1 and 0.3 ns from the beginning of the impact event. The distributions should be compared with the surface morphology schematically illustrated in figure 3.

atomic planes and in the case of Zr as the atoms initially located between the sixth and the 28th atomic planes.

The process of defective atom generation involves the rearrangement of the coordination shells of two neighbouring atoms. One of them takes a 11-fold coordination and the other a 13-fold one. 10-fold and 14-fold coordinations are rarely observed and, in any case, for times on the order of only 0.1 ps. The first defective atoms on the Ni and Zr sides appeared respectively after about 2.4 and 3 ps, corresponding to the surface asperities undergoing the first contact, involving atoms belonging to the 18th Ni and the 28th Zr atomic planes. The successive defective atom pairs appeared in the same planes, close to the previous ones. The distribution of defective atoms is not uniform. This can be clearly seen from figure 7, where the two-dimensional maps of defective atoms at different times are quoted. A comparison of the maps with the initial morphology of the surface indicates that defective atoms appear in positions corresponding to the atomic assemblies at the surface. Successively, defective atoms attain a more uniform distribution.

A direct visualization of the defective atoms in both the Ni and Zr semi-crystals points out that such species arrange according to string-like structures. The number and size of such structures, or clusters, was evaluated by applying the same distance criterion as employed to identify and distinguish defective atoms from 12-fold coordinated ones. Defective atoms are thus regarded as belonging to the same cluster when located at distances shorter than the one corresponding to the first PCF minimum. For the sake of illustration, a small cluster of defective atoms is shown in figure 8. Under the action of shear stresses, defective atoms belonging to a given cluster are continuously replaced by other atoms. A given defective atom belonging to the cluster can leave it and restore its normal coordination while a neighbouring atom becomes defective. A similar behaviour was observed in previous work [19, 20]. Both the size, i.e. the number of defective atoms in the cluster, and the position of the cluster change during the course of the impact event. Defective atoms and their pseudo-linear clusters have indeed a relatively high mobility and migrate under shearing. The dynamics of the defective atom clusters is

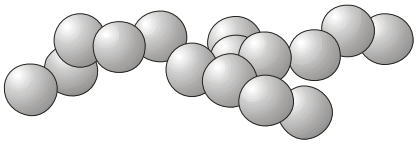

Figure 8. A cluster of 16 Zr atoms with defective coordination. The snapshot refers to the atomic configuration observed after 70 ps from the beginning of the impact event. The atoms are arranged according to a pseudo-linear structure.

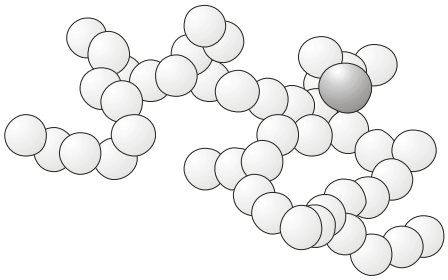

Figure 9. A cluster of 46 defective Ni atoms containing a closed loop extracted from the atomic configuration at about 110 ps. For the sake of clarity, only the atomic species belonging to the cluster are reported, with the exception of a Zr atom, in heavy grey. The latter, not connected to the Ni cluster, is visible close to the loop. Ni atoms are reported in light grey.

relatively complex and mainly governed by branching chain processes. These processes occur according to two different mechanisms. In the first place, two separate clusters can approach closer and closer and finally intersect, thus forming a single larger cluster. Alternatively, defective atoms can proliferate along a certain direction, forming a ramification of the original cluster. In both cases, branching lowers the potential energy of the local atomic arrangement and relieves their atomic strain.

Due to their remarkable linear character, similar defective structures were in previous work regarded as dislocation lines [37]. It is however worth noting that the string-like clusters formed by defective atoms do not correspond generally to actual dislocation lines. Branching chain processes occasionally induce the formation of closed loops of defective atoms, such as the one shown in figure 9. Such loops have very short lifetimes, on the order of 20 ps. Within this time window, however, the loops are seen to roughly correspond to Shockley partial dislocations. The mobility of the loops mirrors the one of defective atoms. The loops appearing on the Ni side of the Ni–Zr interface are seen to glide mainly along the [101] and [110] crystallographic directions. On the Zr side of the interface, the loops are instead seen to glide mainly along the [110] and [210] crystallographic directions. It seems therefore that the loops of defective atoms identifiable with Shockley partials move in accordance with the known glide systems in fcc and hcp lattices.

The results at this point are however only preliminary and further work is required to explore in detail the configurations of defective atoms at the various stages of the collision. The analyses performed to identify the structural characteristics of the clusters of defective atoms are partial and based upon the direct visualization of the clusters, which leaves room for subjective interpretation. The observations here reported must not be intended therefore as conclusive, but only as indicative of the possible formation of dislocations during the course of the impact event.

3.3. The mixing process at the interface

The generation of defective atoms and the associated atomic displacements promote the occurrence of mixing phenomena between the chemical species. Mixing processes are restricted to the interfacial region and take place under far-from-equilibrium conditions.

The thickness Δ of the layer in which the chemical species get mixed can be roughly evaluated as the difference between the z Cartesian coordinates of the Ni and Zr atoms

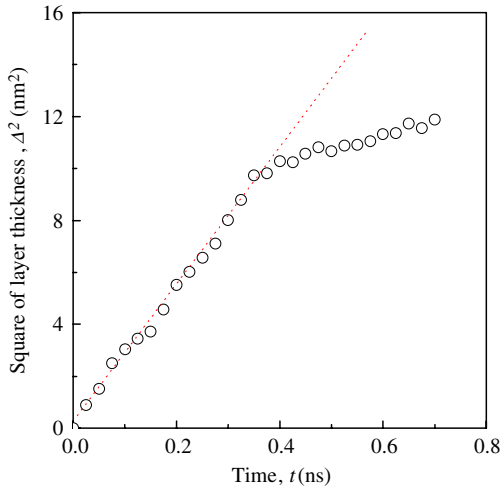

Figure 10. The square of the mixed layer thickness, Δ^2, as a function of the time t. Two approximately linear trends are evident. The line best fitted to the first portion is also shown. The time dependence of Δ is therefore similar to the one observed during thermal diffusion processes.

respectively closer to the Zr and Ni reservoir regions [30]. The quantity Δ then measures the distance of penetration of a chemical species into the lattice of the other. Such distance changes with time, as shown in figure 10, where the square of the thickness Δ is quoted as a function of the time t. The first portion of the curve is remarkably linear. This suggests that during the first stages of the impact the thickening of the mixed layer displays a time dependence analogous to the one observed in the case of conventional thermal diffusion despite the completely different mechanism involved. Such time dependence has however also been observed in other cases in which thermal diffusion is thought to play only a secondary role, the mixing being ruled by shear-induced atomic displacements [14, 19, 20].

A definite change of slope is observed after about 0.35 ns from the beginning of the collision, indicating a change in the mechanism governing the mixing process. At about 0.3 ns the two colliding semi-crystals have indeed attained the configuration in which all the asperities at the surfaces are strongly interacting with each other or directly with the surface of the opposite semi-crystal. At about 0.35 ns, the structure of the surfaces of the semi-crystals has been already significantly perturbed and the system is approaching the configuration in which the two Ni and Zr semi-crystals become strongly compressed one against the other. Under such compressive load, the mobility of the surface species is greatly reduced. The mechanism of high energy ballistic displacement of the Ni and Zr atoms at the surface is then replaced by processes involving a slower rearrangement of the atomic positions. As a result, while the thickness Δ of the intermixed layer amounts to about 3 nm after 0.35 ns, it has increased approximately by only 0.5 nm after an additional 3.5 ns.

Corresponding to the modification of the mechanistic scenario underlying the mixing process at the interface, the apparent diffusion coefficient D_a defined as the slope of the linear portions in figure 10 changes from about 26 nm^2 ns^{-1} to about 6 nm^2 ns^{-1}. It is worth noting that the mobility of the atomic species in the first mechanistic regime is similar to the one observed in the case of interfacial mixing processes induced by the relative sliding of Ni and Zr semi-crystals [19, 20]. In such a case the apparent diffusion coefficient D_a was indeed roughly equal to 23 nm^2 ns^{-1} [19, 20]. As briefly mentioned above, the net decrease of D_a relative to the second mechanistic regime is undoubtedly connected with the densification of the interfacial region and the consequent decrease of the atomic mobility. The D_a value observed of about

6 $nm^2\ ns^{-1}$ is roughly of the same order of magnitude as the ones obtained in previous work focusing on the atomic mobility at a disordered Ni/Zr interface under mechanical loading [30]. The apparent diffusion coefficients D_a obtained in such a case were indeed approximately in the range between 1 and 10 $nm^2\ ns^{-1}$ [30].

All the apparent diffusion coefficient values mentioned above are orders of magnitude larger than the value of about 10^{-14} $nm^2\ ns^{-1}$ experimentally observed [38] and of about 10^{-4} $nm^2\ ns^{-1}$ numerically obtained after the load removal [30]. As supported by both experimental and numerical evidence [30, 38], this means that the mechanical loading is able to enhance the atomic mobility. This means in turn that loading events determine an increase of the excess free volume and the formation of favoured diffusion paths. Under such circumstances, the atomic displacements are not expected to be ruled by conventional diffusive jumps but rather by collective motions. Although a detailed analysis of the local atomic volume has not been carried out, the results obtained in the present work seem to provide further support for such a conjecture.

3.4. The relaxation process

As the simulations proceed, defective atoms gradually approach the reservoir regions containing immobile species. This fact can result in a non-physical evolution of the system and therefore a wrong representation of the processes taking place during the course of the collision event. For this reason, the calculations were stopped after about 0.7 ns. In order to gain information on the possible dynamics of the relaxation processes relieving the strain of local atomic configurations in the absence of mechanical loads, the calculations were then re-started with no normal force acting on the semi-crystals. As the normal force was removed, fast relaxation processes were seen to occur via short-range displacements of atomic species, rarely exceeding a distance of about 0.4 nm. Such processes essentially involved then the coordination shell of nearest neighbours. However, the system is not able to completely remove local strains and rearrange all the configuration of unusually high potential energy. This is mostly a consequence of the effective action of the Nosè thermostat applied to the mobile atoms in the reservoir regions, which is able to remove the kinetic energy present in excess at the interface in times of the order of 0.1 ns. After 60 ps since the removal of the normal force acting on the semi-crystals the apparent temperature of the interfacial region, evaluated by averaging over five atomic planes below the surface on both the Ni and Zr sides, dropped from about 900 K to about 500 K. After an additional 60 ps, the interfacial temperature is only 370 K.

Under such circumstances, the mobility of the atomic species is greatly restricted and long-range displacements of atomic species prevented. This results in the formation of a disordered interfacial layer consisting of mixed Ni and Zr atoms. The disordered layer, about 3.5 nm thick, has an amorphous-like structure, as indicated by the PCF of the interfacial layer quoted in figure 11.

The relaxation processes subsequent to the removal of the normal force take place within a time interval of about 0.4 ns. No significant atomic displacement is observed at longer times as a consequence of the relatively low temperature. According to such findings, the mixed interfacial region is able to keep a disordered arrangement but not to increase its thickness under annealing conditions at 300 K, at least on the timescale explored in the simulations.

Additional simulations have shown that the thickness of the mixed layer undergoes a detectable increase only when a normal force is applied. When the mechanical load was indeed re-applied after the equilibration stage of about 0.4 ns a mixed layer thickness increase of about 1.2 nm in 0.25 ns was observed. The apparent diffusion coefficient was then roughly equal

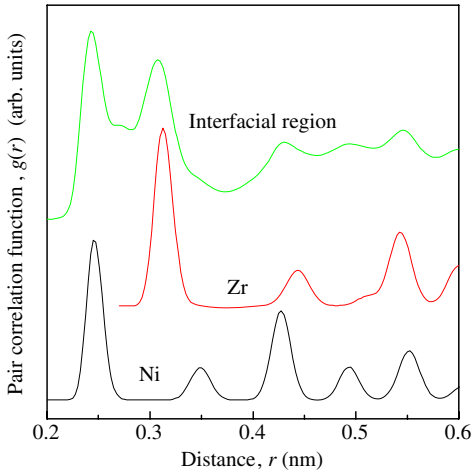

Figure 11. The global PCF $g(r)$ pertaining to the interfacial region approximately enclosed by the 14th Ni and the 24th Zr atomic planes after about 0.6 ns from the removal of the normal force. The PCFs $g(r)$ of Ni and Zr bulk systems at 500 K are also reported for sake of comparison. Although a certain degree of crystalline order is still discernible, the evident crystalline peaks are clearly superposed on two broad halos that can be regarded as indicative of a local amorphization at the interface.

to the one observed during the second impact regime discussed above, further supporting the mechanistic scenario proposed in previous work [30].

4. Concluding remarks

Numerical simulations were carried out to investigate the complex phenomena taking place during the early stages of the collision between two crystalline systems with rough surfaces. The impact event involves initially the surface asperities, at which sudden mechanical loads and shear stresses develop. Atoms correspondingly undergo forced displacements, inducing significant rearrangements of the atomic configurations to relieve local strains. These processes are mediated by atoms with defective coordination. Defective atoms form extended clusters that rapidly evolve in response to local shearing, modifying their number, size and shape. The enhanced mobility of defective atoms promotes the mixing of atomic species. A layer of intermixed species is gradually formed at the interface, the thickness of which increases with time according to a power law similar to the one characteristic of thermal diffusion. In this case, no significant thermally activated mass transport phenomenon is however observed. It appears that atomic displacements are rather due to shearing events.

Thermal displacements are instead observed after the removal of the normal force, when the system undergoes a fast relaxation. Correspondingly, defective atoms relax their coordination shells and recover a normal coordination. The rearrangement of atomic species and the consequent equilibration of local atomic configurations in the mixed layer is however hindered by the atomic size mismatch. The interfacial region therefore keeps its structural disorder, showing an amorphous character. The layer thickness does not increase further unless compressive loads are applied.

Far from being exhaustive, the numerical findings point out the important role played by the shear-induced displacements of atomic species in the formation of a structurally disordered interface. With the present one restricted to the early stages of a single collision event, further

study is necessary to investigate the role of factors such as the roughness of the colliding surfaces in the mechanism of mixing and disordering processes.

Acknowledgments

Financial support has been provided by the University of Cagliari. Professor G Cocco, Dipartimento di Chimica, Università degli Studi di Sassari, is gratefully acknowledged for useful discussions. A Ermini, ExtraInformatica s.r.l., is gratefully acknowledged for technical support.

References

[1] Cahn R W and Haasen P (ed) 1996 *Physical Metallurgy* 4th revised and enhanced edition (Amsterdam: Elsevier Science BV)
[2] Easterling K E and Porter D A 1992 *Phase Transformations in Metals and Alloys* (London: Chapman and Hall)
[3] Kittel C 1996 *Introduction to Solid State Physics* (New York: Wiley)
[4] Heinicke G 1984 *Tribochemistry* (Berlin: Akademie-Verlag)
[5] Butyagin P Yu 1989 *Sov. Sci. Rev. B Chem.* **14** 1
[6] Suryanarayana C 2001 *Prog. Mater. Sci.* **46** 1
[7] Khina B B and Froes F H 1996 *J. Met.* **48** 36
[8] Courtney T H 1995 *Mater. Trans., JIM* **36** 110
[9] Bellon P and Averback R S 1995 *Phys. Rev. Lett.* **74** 1819
[10] Hammerberg J E *et al* 1998 *Physica* D **123** 330
[11] Hoagland R G and Baskes M I 1998 *Scr. Mater.* **39** 417
[12] Bulatov V *et al* 1998 *Nature* **391** 669
[13] Ovid'ko I A and Reizis A B 1999 *J. Phys. D: Appl. Phys.* **32** 2833
[14] Fu X Y *et al* 2001 *Wear* **250** 420
[15] Horstemeyer M F *et al* 2001 *Acta Mater.* **49** 4363
[16] Kadau K *et al* 2002 *Science* **296** 1681
[17] Lund A C and Schuh C A 2003 *Appl. Phys. Lett.* **82** 2017
[18] Levitas V I 2004 *Phys. Rev.* B **70** 184118
[19] Delogu F and Cocco G 2005 *Phys. Rev.* B **71** 144108
[20] Delogu F and Cocco G 2005 *Phys. Rev.* B **72** 014124
[21] Johnson W L 1986 *Prog. Mater. Sci.* **30** 81
[22] Meng W J *et al* 1987 *Appl. Phys. Lett.* **51** 1693
[23] Gosele U and Tu K N 1989 *J. Appl. Phys.* **66** 2619
[24] Highmore R J 1990 *Phil. Mag.* B **62** 455
[25] Greer L 1990 *Phil. Mag.* B **61** 525
[26] Yavari R and Desrè P J 1992 *Mater. Sci. Forum* **88–90** 43
[27] Massobrio C *et al* 1990 *Phys. Rev.* B **41** 10486
[28] Rosato V *et al* 1989 *Phil. Mag.* A **59** 321
[29] Ducastelle F 1970 *J. Physique* **31** 1055
[30] Mura P *et al* 1994 *Phys. Rev.* B **50** 2850
[31] Allen M P and Tildesley D 1987 *Computer Simulation of Liquids* (Oxford: Clarendon)
[32] Nosè S 1984 *J. Chem. Phys.* **81** 511
[33] Parrinello M and Rahman A 1981 *J. Appl. Phys.* **52** 7182
[34] Delogu F *et al* 2000 *Phil. Mag.* A **81** 1917
[35] Delogu F 2006 *Mater. Sci. Eng.* A **416** 33
[36] Casas-Vazquez J and Jou D 2003 *Rep. Prog. Phys.* **66** 1937
[37] Gomez L *et al* 2003 *Phys. Rev. Lett.* **90** 095701
[38] Mazzone G *et al* 1990 *Phys. Rev. Lett.* **65** 2019